JOURNAL OF AGRICULTURAL AND FOOD CHEMISTRY

New Approach for Characterization of Gelatin Biopolymer Films Using Proton Behavior Determined by Low Field ^{1}H NMR Spectrometry

YOUNG-TECK KIM,[†] YOUNG-SHICK HONG,[‡,§] ROBERT M. KIMMEL,*[,†] JEONG-HAE RHO,[||] AND CHERL-HO LEE[‡]

Department of Packaging Science, Clemson University, Clemson, South Carolina 29634, School of Life Science and Biotechnology, Korea University, Seoul 136-701, Korea, and Korea Food Research Institute, Sungnam-si, Kyunggi-do 463-420, Korea

The behavior of protons in biopolymer films (BFs) formed with gelatin, water, and glycerol was investigated at various relative humidities (RHs) and concentrations of glycerol using a low field ^{1}H NMR spectrometer. At a RH of approximately 0%, the distributed spin–spin relaxation times (T_2) of protons in BFs showed two components: a rapidly relaxing proton with the shortest T_2 derived from protons in the rigid backbone of the gelatin polymer such as CH_1–, CH_2–, and CH_3–, and a slowly relaxing component with longer T_2 from protons of the functional groups in amino acid residues in gelatin such as –OH, –COOH, and $–NH_3$. These two components are referred to as nonexchangeable (T_{2N}) and exchangeable protons (T_{2E}), respectively, indicating the different mobility of the protons. The T_{2E} increased as RH increased indicating the increase in relative mobility of protons due to the larger free volume in the BF matrix. Above a RH of 33%, the slowest relaxing component was found in all BFs and referred to as hydration–water protons (T_{2W}) with the highest relative mobility of all protons in the films. It suggests that the free volume in BFs can be formed above a RH of 33% in the absence of glycerol. The behaviors of T_{2N}, T_{2E}, and T_{2W} reveal the formation of free volume in the BF matrix associated with the presence of plasticizers (water and glycerol). The T_2 behavior in BFs is consistent with the behavior of spin–lattice relaxation (T_1). Our result is the first attempt to characterize using low field ^{1}H NMR technology how all protons in a film matrix behave and to develop correlations between proton mobility and free volume in protein-based BFs plasticized with water and glycerol.

KEYWORDS: Gelatin film; low field ^{1}H NMR; biopolymer film; hydration; plasticizer; spin–spin relaxation time (T_2); spin-lattice relaxation time (T_1); CONTIN algorithm; CPMG sequence; Hahn's SE sequence

INTRODUCTION

Biopolymer films are widely applied in research areas such as biochemistry, biopolymers, food science, and nanotechnology because of the chemical and physical advantages embodied in their functionality and environmental friendliness.

Gelatin is a natural protein-based biopolymer product obtained from the structural and chemical degradation with very dilute acid of collagen isolated from animal skin and bones (*1*). Recently, gelatin biopolymers have been widely studied mainly due to their biodegradability and usefulness for commercial purposes (*2*). One especially useful feature is the ability to simply form thin film layers similar to petroleum-derived plastic films (*1–3*). The food, pharmaceutical, and photographic industries are the main users of gelatin biopolymers, which also have several other technical applications. Its most frequent uses in the biomedical field include hard and soft capsules, microspheres, sealants for vascular prostheses, wound dressings, and adsorbent pads for surgical use, as well as three-dimensional tissue regeneration (*1–5*). Gelatin biopolymer films containing greater triple-helix content swell less in water and are consequentially much stronger. Their structure has been modified for various reasons (*3–7*) through chemical or physical cross-linking, using enzymes (e.g., transglutaminase) or chemical agents (e.g., glutaraldehyde) (*6*).

The structure of gelatin biopolymers can be stabilized by inter- and intramolecular hydrogen bonds, hydration water forming hydrogen bond bridges between peptide residues, close van der Waals interactions between imino acid residues, the periodicity of Gly, the relatively high content of the imino acid residues imposing conformational restrictions, and hydroxyl groups of Hyp (*8–14*).

* Corresponding author: Robert M. Kimmel, E-mail: kimmel@clemson.edu, Tel: 864-656-6534.
[†] Clemson University.
[‡] Korea University.
[§] Author Young-Shick Hong has equivalently contributed on this paper as a first author.
[||] Korea Food Research Institute.

10.1021/jf071092f CCC: $37.00
Published on Web 12/04/2007

Many commercial articles (e.g., packaging film, pharmaceutical capsules or lens, and photographic biopolymer film) using biopolymers as a main component are at a relatively low level of water content and contain various minor components (e.g., plasticizers). To characterize properties such as their mechanical and rheological properties, it may be useful to understand the molecular dynamics of the biopolymer, water, and other constituents.

Low field proton (^{1}H) NMR spectroscopy has potential as a method to determine the molecular dynamics and physical structure of biomaterials or polymers (*15–20*) and foods (*21–26*) through measurements of the spin–lattice (T_1) and spin–spin (T_2) relaxation times. In these previous studies, it was reported that hydrated samples have a complex NMR relaxation behavior due to the effect of magnetization transfer between water and polymer protons through chemical exchange or cross-relaxation and exhibit other complex behavior from the existence of multiple correlation times for each exchanging species. However, these studies on proton mobility have been performed with only highly hydrated samples such as collagen (*27*) and gelatin gels (*28*). Therefore, in order to understand the various properties of biopolymers using the spin–lattice (T_1) and spin–spin (T_2) relaxation times, the various proton behaviors of biopolymer should be fully characterized at various levels of water content and minor components (plasticizers).

In our study, the complicated chemical and dynamic interactions revealed by proton behavior in biopolymer films formed with gelatin, water, and glycerol were characterized using a low field ^{1}H NMR. A structural matrix model of gelatin biopolymer film at various environmental conditions is proposed in terms of free volume and proton mobility at the molecular level.

EXPERIMENTS

Sample Preparation. Gelatin solutions for films were prepared by dissolving 10 g of gelatin (type B from limed bone, gelatin 200 Nitta Gelatin, Inc. (Osaka, Japan)) and 0–5 g of glycerol (Sigma, St. Louis, MO) in 100 mL of distilled water. The pH of this solution was about 4.7. The gelatin solution was cast on flat, level Teflon-coated glass plates (25 × 25 cm). Films were peeled from the plates after drying at room temperature for 20 h.

Gelatin film specimens were conditioned in desiccators for over 3 days at 11% RH (relative humidity) to reduce the initial moisture content. These predried films (about 3 g each) were moved to desiccators at 0% RH, 23% RH, 33% RH, 53% RH, 69% RH, 81% RH, and 93% RH for over 10 days and were equilibrated, until no further weight changes were observed. The relative humidity in the desiccators was adjusted using saturated salt solutions of known relative vapor pressures ranging from 0 to 0.93: P_2O_5, approximately 0; KCH_3CO_2, 0.23, $MgCl_2$, 0.33; $Mg(NO_3)_2$, 0.53; KI, 0.69; $(NH_4)_2SO_4$, 0.81; and KNO_3, 0.93.

NMR Measurements. The measurements of the proton relaxation curves were carried out on a 20 MHz ^{1}H NMR Minispec (Bruker, Germany) with a 10 VTS probe and 10 mm diameter sample tubes. The gelatin films equilibrated in desiccators containing saturated salt solutions were cut into rectangular pieces of regular size, moved to NMR tubes (7 in. length, 10 mm diameter; Wilmad, Buena, NJ) and then immediately returned to the desiccators. After an additional equilibration for 48 h, these NMR tubes containing gelatin films were covered with Parafilm and a tube cap. All measurements were made at 25 ± 1 °C.

Spin–lattice relaxation times (T_1) were measured using an inversion–recovery (IR) sequence, [180°–τ–90°], with τ varying logarithmically from 1 to 2000 ms over 30 steps. The obtained FID (free induction decay) curves were fitted by a monoexponential decay function.

Spin–spin relaxation times (T_2) were measured by applying the Carr–Purcel–Meiboom–Gill (CPMG) (*29*) sequence with 90−180° pulse space of 40 μs and with 500 data points, 90°–τ–[180°–2τ–(echo)]$_n$. To measure a short T_2 spin–spin relaxation times were also obtained using the Hahn's spin–echo (SE) sequence (*30*) with 10 μs of pulse space between 90° and 180°, [90°–τ–180°–τ–echo]. The pulse lengths of each pulse were 2.60 and 4.90 μs, respectively. In general, to get each component of spin–spin relaxation time the FID curves were fitted by a multiexponential function.

Spin–Spin Relaxation (T_2) Data Analysis. Spin–spin relaxation decay curves in gelatin films obtained in our studies were inverted into corresponding distributions of relaxation times using the CONTIN algorithm (*31*). CONTIN approximates a solution to the inverse Laplace transform applied to the decay of peak intensity and produces a continuous distribution of relaxation components. This program has been successfully applied to the analysis of not only relaxation times obtained using low field ^{1}H NMR in fresh and frozen–thawed cod but also diffusion coefficient distributions obtained by PFG-NMR in humic and fulvic acids, polymer, phospholipids vesicles, and polymer–surfactant systems (*32–35*), as well as of stress relaxation times obtained by a texture analyzer in food gels, including gellan, carrageenan, whey protein, and gelatin gels (*23*).

The continuous distributions of spin–spin relaxation times were calculated by the CONTIN package (Bruker, Germany) defined by the following equation

$$g_i = \sum_{j=1}^{m} f_i \exp\left(\frac{-t_i}{T_{2j}}\right) \quad (1)$$

where g_i is the amplitude of the exponential distribution at time t_i, f_i is the pre-exponential multiplier of the distribution, and T_{2j} is the spin–spin relaxation time of the jth component. The distributions of T_2 of about 10 μs by Hahn's SE sequence were obtained by a proper back extrapolation after assuming them to be Gaussian because the dead time of the Minispec was 10 μs.

Gas Permeability. A MOCON Permatran-W3/31 water vapor permeation measurement system with an IR detector was used to measure and analyze the water vapor transmission rate. The oxygen transmission rate was determined in an OX-TRAN 2/20 (Mocon, Inc., Minneapolis, MN) at 25 °C and 50% RH conditions. Each test was done according to ASTM F1249 (*36*) and ASTM D3985 (*37*), respectively.

RESULTS AND DISCUSSION

Relaxation Times and Their Distributions. Generally, the decay of spin–spin relaxation time using the CPMG sequence was found to be monoexponential. However, the spin–spin relaxation time curve obtained using Hahn's SE sequence was found to be bi- and triexponential in the absence and presence of water, respectively. Furthermore, both spin–spin relaxation times calculated in the decay curve using the SE and CPMG sequence were analyzed using a continuous distribution model in the CONTIN algorithm (*31*) as shown in **Figures 1–3**. The distributed components showed a good agreement with components obtained by fitting the relaxation decay curves.

Figure 1 shows the effect of glycerol on the spin–spin relaxation time at a RH of approximately 0, analyzed using a continuous distribution model with Hahn's SE sequence in BFs. In the absence of water, the distributed analysis reveals the presence of two components for all samples. These two components in gelatin films are characterized by short T_2 relaxation time indicating an immobile and by longer T_2 indicating relatively more mobile protons.

It has been suggested that the slow-relaxing component in gelatin at low water content arises from hydration water, together with mobilized low molecular weight oligopeptides and possibly the extremities of gelatin chains, and the fast-decaying component is from rigid gelatin protons (*28*). In water-rich biopolymer systems a model involving four proton pools has also been assumed, each associated with its own intrinsic proton spin–spin

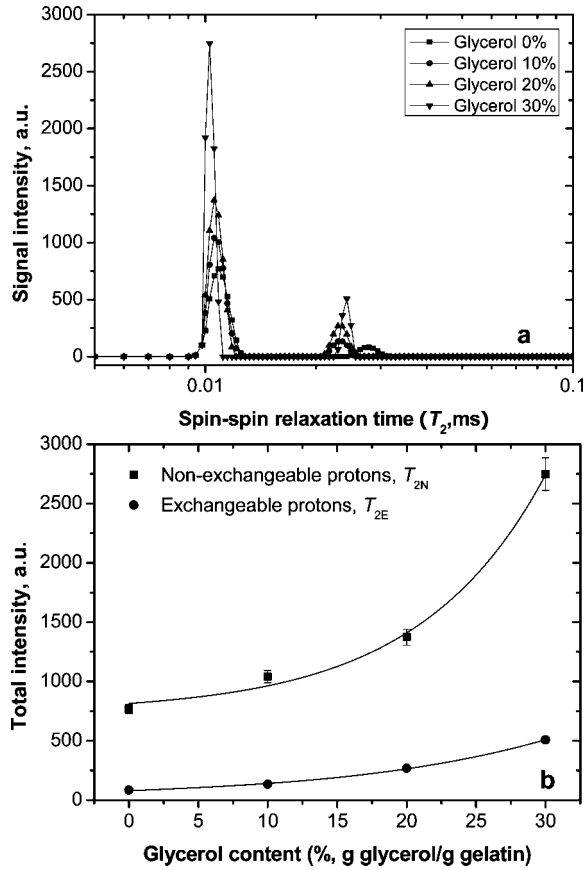

Figure 1. The continuous distribution of spin–spin relaxation times (T_2) (**a**) and changes in total intensity of nonexchangeable protons (T_{2N}) and exchangeable protons (T_{2E}) (**b**), obtained using Hahn's SE sequence in BFs containing varying glycerol concentrations from 0 to 30% (0.3 g of glycerol/g of gelatin) in the absence of water at 25 °C. Note that T_{2N} times of about 10 μs were obtained by a back extrapolation to Gaussian.

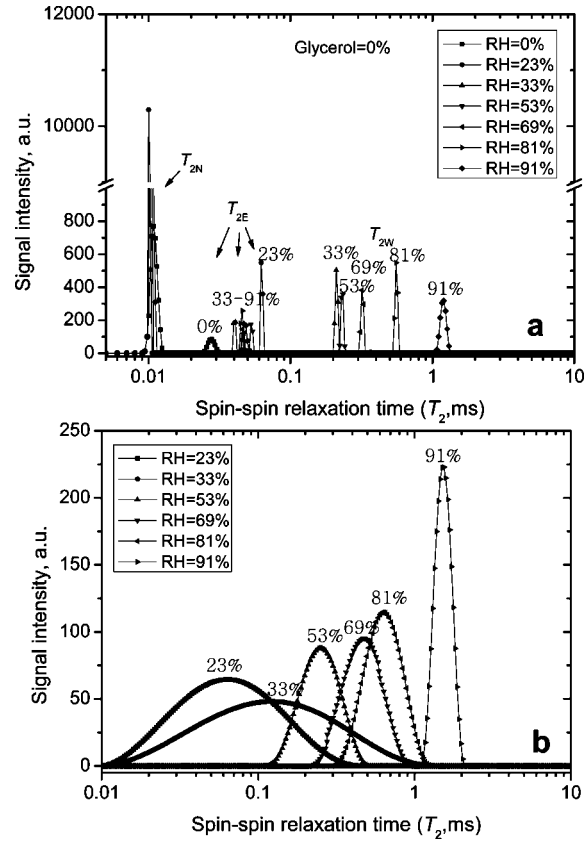

Figure 2. The continuous distributions of spin–spin relaxation times (T_2) obtained using Hahn's SE sequence (**a**) and the CPMG sequence (**b**), with increasing relative humidity in gelatin films in the absence of glycerol at 25 °C. Note that the proton corresponding to a high mobility using the CPMG sequence (**b**) at a RH of approximately 0 was not detected due to a very weak signal, even though the number of scans of acquisition parameters was increased.

and spin–lattice relaxation times: (1) bulk water whose motion is essentially unperturbed by biopolymer interactions; (2) hydration water whose correlation times are lengthened by interaction with the biopolymer; (3) exchangeable protons in gelatin structure; (4) nonexchanging protons in gelatin structure (*38*, *39*). In dried chitosan polymer, a fast relaxing component attributed to the polymer lattice and a slow relaxing component from acetyl groups have been also found (*17*).

In our studies, the fast relaxing component with the shortest T_2 (T_{2N}) is considered to be protons from the nonexchangeable rigid backbone of gelatin such as –CH, $-CH_2$, and $-CH_3$, and the slow relaxing component (T_{2E}) is considered to be protons from the exchangeable side chains of amino acid residues such as –OH, $-NH_3$, and –COOH or to be protons in water bound to the side chains. In the absence of glycerol, the fast and slow relaxing components had T_2 values of 10 ± 0.5 μs and 27 ± 1 μs, respectively, as shown in **Figure 1a**. The shortest T_{2N} value of 10 μs obtained in this study was in good agreement with that of 12 μs obtained from gelatin molecules using 20 MHz ^{1}H NMR (*28*) and solid-state 300 MHz ^{1}H NMR studies (*40*). These short T_2 values ranging from 11 to 17 μs corresponding to protons in solidlike components have also been reported in wheat dough (*41*) and soy protein isolate-based film (*42*). As shown in **Figure 1b**, in the absence of water the signal amplitudes corresponding to both T_{2N} and T_{2E} increase as glycerol concentration increases. This suggests that the signal amplitudes of nonexchangeable rigid protons and exchangeable protons both in glycerol and gelatin polymer contribute to the amount of the fastest relaxing component and the slowest relaxing component, respectively.

Nonexchangeable Protons. The T_{2N} values (time) of rigid protons on the gelatin backbone in the films did not change significantly with increasing relative humidity (RH) to 91%, as shown in **Figure 2**. In addition, T_{2N} values of the rigid protons in gelatin biopolymer films were not changed with increasing water and glycerol content, even in the range of from 4 to 45 °C (data not shown). However, the amplitude of intensity corresponding to nonexchangeable protons in the films increased from 768 to 10293 (arbitary unit, a.u.) as the RH decreased from 23% to 0% (**Figure 2a**). The intensities at over 23% RH were approximately constant at reduced values of around 4653. Note that the amplitude intensity of T_{2N} in **Figure 2b** was not considered in our discussion due to the limitation of CMPG sequence analysis. It is generally used for the analysis of mobile proton distribution among various T_2.

On the basis of the multilayer water model (*28*), the rigidity of the polymer chains will also increase as the plasticization effect of multilayer water is lost. This is because the removal of multilayer water will increase the lifetime of the water molecules adsorbed at the polymer binding sites, converting them from "mobile" to "solidlike" protons. This means that the water fraction is associated with the fast relaxing "rigid" proton pool at 15% water content in the gelatin gel (*28*). For this reason, the rigidity or flexibility of biopolymer films containing only

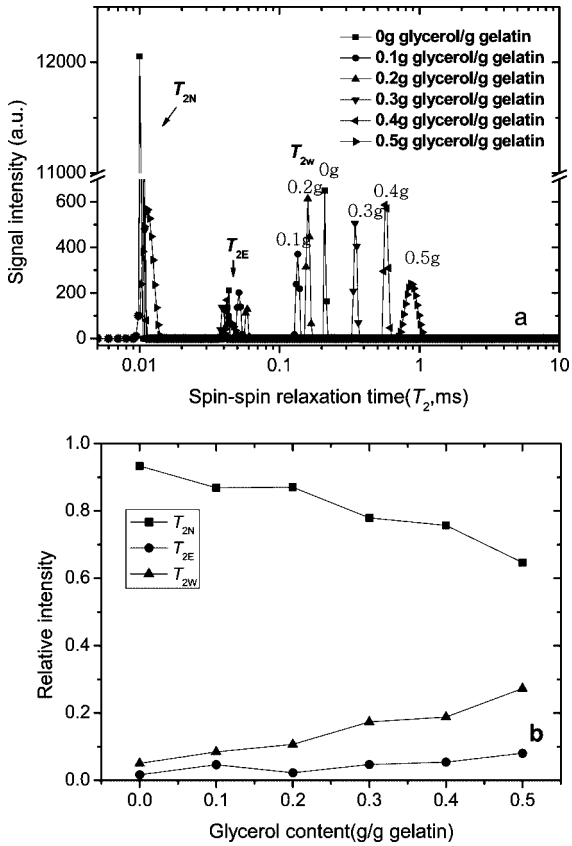

Figure 3. The continuous distributions of spin–spin relaxation (T_2) obtained using Hahn's SE sequence (**a**) and changes in the relative intensity (**b**), with increasing glycerol concentration in gelatin films at RH = 53%. Note that the distributed values corresponding to T_{2N} are not indicated because there was no significant difference.

water can be correlated with the intensity amplitude or spin density of rigid protons of the biopolymer.

In such a case, the rigid protons in glycerol affect the signal intensity of the rigid protons in gelatin. Consequently, the decrease in the total intensity of the rigid protons above RH 33%, compared to the intensity of that at 23% RH, strongly indicates that solidlike water molecules or bound water to exchangeable protons in BFs are dominant on the multilayer at RH 23% and the water molecules actively plasticize the rigid gelatin biopolymer chains.

Note that many researchers have not reported the rigid protons in polymers because they used the CPMG sequence to obtain the more mobile protons in the high water content in the polymer gel and also the interpulse space time between 90° and 180° pulses in Hahn's SE sequence was not short enough to refocus magnetization from nonexchangeable protons (*19*).

Exchangeable Protons. In contrast to T_{2N}, the water content level affects the values of T_{2E}. With an exception at 23% RH, the value of T_{2E} measured by the SE sequence clearly increases from 27 to 62 μs as RH increased from 0 to 91% in the absence of glycerol because the water molecules serves as a plasticizer (**Figure 2** and **3a**). This observation was confirmed by the CPMG sequence to compensate for the effects of field inhomogeneity as shown in **Figure 2b**. The T_{2E} at RH 23% was the longest among all T_{2E} values. Moreover, the most mobile protons (T_{2w}, water protons in hydrated pools which are explained in the next section) at 23% RH condition were not observed in the range of 228 μs to 1.2 ms. This implies that, at the 23% RH condition, the exchangeable protons were not separated into the water protons in hydrated pools, perhaps due to insufficient

Table 1. Spin–Lattice Relaxation Time (T_1) of Water in Gelatin Films in the Absence of Glycerol with Increasing RH (%)

	0 RH	23 RH	33 RH	53 RH	69 RH	81 RH	91 RH
T_1 (ms)	70 (±50)	85 (±2)	58 (±2)	56 (±2)	54 (±2)	49 (±2)	50 (±1)

water content to form the free volume in BFs. This is evidence of the dominant existence of solidlike water molecules in the multilayer water model (*28*) at 23% RH. It also suggests that the dramatic change of the structural matrix of BFs, such as the formation of free volume induced by water molecules, occurs at conditions where RH is greater than 33%. This effect of water on free volume for polymer motions has been reported in starch (*24, 43, 44*). These results showed that there are strong interactions between water molecules and the polar groups on the chains through hydrogen bonds in BFs. A similar phenomenon was observed in the T_1 value at various RH conditions (**Table 1**), implying that the structural change in free volume begins between the 23% and the 33% RH conditions.

Hydration Water Protons. At RH of 33% and over, the slowest relaxing components characterized by the longest spin–spin relaxation time were successively observable at the wide range of 228 μs to 1.2 ms, as shown in **Figure 2**. It represents the highest mobile protons in BFs. Since the slowest relaxing components showing the highest T_2 of over 200 μs were not found in the absence of water, these components can be primarily considered to be derived from water protons in hydration pools (T_{2w}). On the basis of this phenomenon that the slowest relaxing components (T_{2w}) are derived from hydration water protons, the different values of T_{2w} can represent different degrees of molecular association between neighboring hydrated water protons. The formation of free volume is driven through swelling of the protein networks. The free volume induced by water should influence various physical properties of biopolymer films such as mechanical properties and gas permeability (*45*).

The Dynamic Properties of BF with Varying Glycerol Content. Figure 3a shows the proton behavior of spin–spin relaxations in BF with increasing glycerol concentration from 0.1 to 0.5 g (w/w, g/g of gelatin) at 53% RH. On the basis of the characterization of various T_2, the value of T_{2E} increased from 43.4 ± 1 μs to 58.8 ± 1 μs as the glycerol concentration increased from 0 to 0.2 g in the film (**Table 3**). This indicates the presence of a plasticizing effect. It is of interest that the values of $T_{2W}$with 0.1 and 0.2 g of glycerol were shorter than those obtained without glycerol. This suggests that the amount of hydrated water for the formation of free volume induced by water hydration is decreased with increasing glycerol concentration up to 0.2 g due to stronger interactions between hydrated water and the protons of the glycerol.

Above 0.3 g of glycerol, the values of T_{2E} were observed in the range of approximately 42 μs and the values of T_{2W} increased from 346 ± 3 μs to 887 ± 8 μs. This suggests that the exchangeable protons (T_{2E}) and hydrated water protons (T_{2W}) were completely separated. Therefore, it showed higher mobility of T_{2W} than those below 0.3 g.

The relative intensities of T_{2N} decreased but T_{2E} and T_{2W} increased with increasing glycerol concentration as shown in **Figure 3b**. This indicates that the rigidity of gelatin biopolymer films decreased with increasing glycerol. This is in good agreement with the observations that the increase of the plasticizer concentration in the film-forming solutions produces less stiff and rigid but more extensible biopolymer films due to the reduction of inter- and intramolecular association between the biopolymer chains (*46*).

Table 2. Spin–Lattice Relaxation Time (T_1) of Water in Gelatin Films with Increasing Glycerol at Approximately 53% RH

	0 g of glycerol/g of gelatin)	10 g of glycerol/g of gelatin)	20 g of glycerol/g of gelatin)	30 g of glycerol/g of gelatin)	40 g of glycerol/g of gelatin)	50 g of glycerol/g of gelatin)
T_1 (ms)	56 (±1)	57 (±1)	51.7 (±1)	41.6 (±0.5)	37.1 (±0.4)	35.2 (±0.5)

Table 3. Water Vapor Permeability ($\times 10^{-6}$ g m^{-1}day^{-1}) and Oxygen Permeability ($\times 10^{-6}$ cm^3 m^{-1} day^{-1}) of Gelatin Films Plasticized with Various Glycerol Concentrations at RH = 50% and 23 °C

glycerol (%, g/g gelatin)	water vapor permeability, $\times 10^{-6}$cm^3 m^{-1} day^{-1}	oxygen permeability
0	29.62 ± 1.24	9.77 ± 0.79
10	7.79 ± 0.12	2.94 ± 1.09
20	5.28 ± 0.15	0.78 ± 0.29
30	8.56 ± 0.27	1.28 ± 0.04
40	13.75 ± 0.87	2.65 ± 0.08

These behaviors of each proton pool were also consistent with the changes in the relative proton populations of mobile and immobile protons in gelatin gels below a water content of 15% (wet basis) (*28*) because the water like glycerol also serves as a plasticizer in the films.

The Spin–Lattice Relaxation Time. The spin–lattice time (T_1) is characterized by the recovery of longitudinal magnetization using the IR sequence. **Tables 1** and **2** show the evolution of the spin–lattice relaxation times (T_1) at various relative humidities in the absence of glycerol and with various glycerol concentrations at RH = 53%. The relaxation decay curve for spin–lattice relaxation time was found to be a single exponential for all film samples studied. Although the repetition time was significant enough to measure the T_1 only at RH = 0%, the value of T_1 was undetectable due to the weak water signal. For this reason, it was assumed that the relaxation for T_1 in BF corresponds only to the dynamics of water proton pools. This assumption was consistent with the suggestion that the reduction in spin–lattice relaxation times of the starch samples containing 18% D_2O occurs primarily as a consequence of the water motion rather than through the mobility of starch (*47*).

To better understand the T_1 evolution, the properties of the spin–lattice relaxation have to be considered. The spin–lattice relaxation rate ($R_1 = 1/T_1$) is proportional to the gyromagnetic ratio, the mean-squared value of the local magnetic fields, and the spectral density at the NMR frequency. The magnetic field generated by a nucleus having a magnetic moment from a distance is in inverse proportion to the distance between nuclei located in intermolecular regions (*48*). Its rate is related to linear combinations of the spectral density functions $J^{(0)}(\omega)$, $J^{(1)}(\omega)$, and $J^{(2)}(\omega)$, which take the form

$$J^{(i)}(\omega) = \frac{k_i \tau_c}{r_{ij}^6 (1 + \omega \tau_c)} \quad (2)$$

where k_i is a constant that depends on whether $i = 0$, 1, or 2. The significant term for discussion is the rotational correlation time, τ_c. Although τ_c does depend on the inherent rate at which nuclear magnetic dipoles experience rotation, it also depends on the motions of other parts of the molecule to which it is attached. Relatively immobile molecules, such as those in solids, have relatively longer periods over which adjacent nuclei can interact and dephase or exchange energy with neighboring nuclei. Thus, these nuclei show short T_1 having relatively long correlation times and fast relaxation rates. Nuclei on relatively mobile molecules have rapid motions and thus do not have long periods over which they are influenced by neighboring nuclei. These nuclei show a long T_1 having relatively short correlation times and slow relaxation rates. Therefore, the spin–lattice relaxation rate (R_1) of the nuclei becomes inversely proportional to the distance between the nuclei (*48*).

For this reason, T_1 is very sensitive to the separation between nuclei and hence to the molecular structure (*49*). For example, the decrease of the T_1 values in wheat dough with long mixing time compared with that with short mixing time indicated a combined effect of decreases of intermolecular spacing and water mobility in the sample (*41*). The decrease in T_1 in the BFs was in good agreement with behavior in soy protein isolate (SPI) based film (*42*) as the water and glycerol content increase, although the minimum T_1 with increasing RH and glycerol concentration was not found in this study compared with reports in other film studies (*50, 51*). On the basis of these reports and the concept of dependency of T_1 on the distance between neighboring water molecules, the decrease in T_1 in our studies with increasing glycerol concentration indicates that glycerol stabilizes the film structure because of the increase of mobility of the water between the gelatin molecules and hydroxyl groups in glycerol. Furthermore, as the RH increases, the stabilization of the film can be evaluated by increasing its plasticization. The plasticization depends on the plasticizers such as glycerol and water. The decreases of T_1 with increasing glycerol and water content under study indicate an increase of mobility of the water and then show an increase of the plasticization of the film. The decreases in T_1 with increasing RH and glycerol content were most dramatic between 23% and 33% RH and between 20% and 30% glycerol as shown in **Tables 1** and **2**, respectively. These phenomena are in good agreement with observations of the changes in the T_{2E} values between 23% and 33% RH and between 20% and 30% glycerol. These results were in excellent agreement with findings that T_1 values decreased with the free volume enhanced in *N*-alkyl chitosan-based hydrogels (*52*).

Proposed Model Structure of Gelatin Biopolymer Films (BFs) Plasticized by Water and Glycerol. On the basis of our observations, a model structure of biopolymer film in terms of free volume and rigidity of BF can be proposed, as shown in **Figure 4**. Red balls indicate oxygen atoms, white balls indicate hydrogen atoms, gray balls indicate carbon atoms, and blue balls indicate nitrogen atoms. The exchangeable proton pools in the gelatin biopolymer interact with hydrated water pools which are indicated as the highest T_2(T_{2W}). This can produce a multilayer of water (*28*) in the biopolymer. There is a large cavity between neighboring gelatin chains at 0% RH due to the extreme dryness of the biopolymer, indicating the large free volume and low flexibility of the BF. It is in good agreement with another study (*53*) which has shown the humidity dependence of oxygen permeability coefficient and free volume hole size for EVOH. Between 0% RH and 23% RH, the exchangeable protons (T_{2E}) were not separated into T_{2W}, supporting the presence of a multilayer of water (*28*) on the gelatin biopolymer. Above 33% RH, the exchangeable protons were clearly separated into a more mobile fraction corresponding

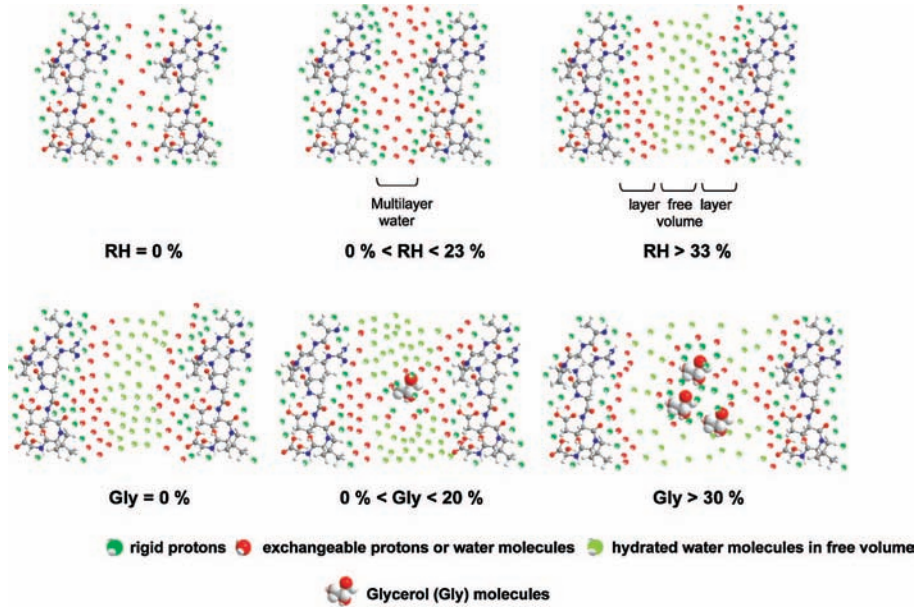

Figure 4. Proposed structural model of biopolymer film for producing free volume with increasing relative humidity (RH) in gelatin biopolymer films in the absence of glycerol and with increasing glycerol concentration at RH = 53%, using spin–spin and spin–lattice relaxation times results in terms of free volume. Green balls and red balls represent the rigid protons in the biopolymer (gelatin) backbone and exchangeable water molecules interacting with rigid protons, respectively. Dark green balls represent relatively free water molecules which induce free volume in the matrix of biopolymer film. Note: At 0% RH, the structure of BFs may be extremely dependent on the drying process of the biopolymer, giving the highest free volume between gelatin molecule aggregations. Glycerol structure has been magnified for illustration purpose.

to T_{2W}. This indicates the presence of a larger free volume between gelatin biopolymer chains and higher flexibility of the BF due to the plasticizing or swelling effect of water. This proton behavior of $T_1$and T_2 corresponding to free volume and flexibility could be confirmed by gas (oxygen and water vapor) permeability (**Table 3**). As shown in **Table 3**, the oxygen and water vapor permeabilities were lowest at 0.2 g of glycerol concentration in gelatin biopolymer film. It is in very good agreement with our proposed model structure assumption corresponding to the free volume and flexibility induced by water.

With increasing glycerol concentration up to 20% (w/w, g/g gelatin), the values of T_{2E} increased while the values of T_{2W} decreased due to the interaction between exchangeable and water protons, and protons of glycerol. Above a glycerol concentration of 30%, the change of T_{2E} was not observed while the T_{2W} values continuously increased. This indicates the increase in the free volume.

Conclusions. With fast measurements of T_1 and T_2 of BFs in the presence of plasticizers (e.g., water and glycerol), we were able to understand and propose the chemical and physical interactions between gelatin biopolymer films and plasticizers as well as the structural matrix of gelatin biopolymer films at various conditions. On the basis of our characterization of spin–spin relaxation and spin–lattice relaxation times in BFs, the chemical and physical properties of other biopolymers containing components such as plasticizers could be predicted with a pulse ^{1}H NMR. For example, it means that this technology can be an alternative way to verify the physical properties of biopolymer film such as gas diffusion rate or mechanical properties based on free volume and flexibility. Thus, we expect that this low field NMR technology can be effectively applied to various research fields (e.g., biomedical engineering (*54*), pharmaceutics (*54*), and nanotechnology (*55*)) with other complementary technology such as PGFNMR or NMR relaxation dispersion (*32*–*35*) in order to understand the characteristics of biopolymers at various conditions at the molecular level.

LITERATURE CITED

(1) Nimni, M. E.; Cheung, D. T.; Strates, B.; Kodama, M.; Sheikh, K. *Collagen*; CRC Press: Boca Raton, FL, 1988; Vol. 3, p 1–38.
(2) Otani, Y.; Tabata, Y.; Ikada, Y. *Biomaterials* **1998**, *19*, 2091–2098.
(3) Rose, P. J.; Mark, H. F.; Bikales, N. M.; Overberger, C. G.; Menges, G.; Kroschwitz, J. I. *Encyclopedia of Polymer Science and Engineering*, 2nd ed.; Wiley Interscience: New York, 1987.
(4) Esposito, E.; Cortesi, R.; Nastruzzi, C. *Biomaterials* **1995**, *20*, 2009–2020.
(5) Digenis, G. A.; Gold, T. B.; Shah, V. P. *J. Pharm. Sci.* **1994**, *83*, 915–921.
(6) Babin, H.; Dickinson, E. *Food Hydrocolloid* **2001**, *15*, 271–276.
(7) Bigi, A.; Panzavolta, S.; Rubini, K. *Biomaterials* **2004**, *25*, 5675–5680.
(8) Brodsky, B.; Ramshaw, J. A. M. *Matrix Biol.* **1997**, *15*, 545–554.
(9) Lazarev, Y. A.; Grishkovsky, B. A.; Kromova, T. B.; Lazareva, A. V.; Grechishko, V. S. *Biopolymers* **1992**, *32*, 189–195.
(10) Bhatnagar, R. S.; Pattabiraman, N.; Sorensen, K. R.; Langridge, R.; Macelroy, R. D.; Renugopalakrishnan, V. *J. Biomol. Struct. Dyn.* **1988**, *6*, 223–233.
(11) Veis, A. In *The Science and Technology of Gelatin*; Horecker, B., Kaplan, N. O., Sheraga, H. A., Eds.; Academic Press: New York, 1964.
(12) Kersteen, E. A.; Raines, R. T. *Biopolymers* **2001**, *59*, 24–28.
(13) Melacini, G.; Bonvin, A. M. J. J.; Goodman, M.; Boelens, R.; Kaptein, R. *J. Mol. Biol.* **2000**, *300*, 1041–1048.
(14) Holmgren, S. K.; Taylor, K. M.; Bretscher, L. E.; Raines, R. T. *Nature* **1998**, *392*, 666–667.
(15) Moody, J.; Xia, Y. *J. Magn. Reson.* **2004**, *167*, 36–41.
(16) Saalwachter, K. *J. Am. Chem. Soc.* **2003**, *125*, 14684–14685.
(17) Capitani, D.; Crescenzi, V.; De Angelis, A.; Segre, A. *Macromolecules* **2001**, *34*, 4136–4144.
(18) Steren, C.; Monti, G.; Marzocca, A.; Cerveny, S. *Macromolecules* **2004**, *37*, 5624–5629.

(19) McConville, P.; Whittaker, M.; Pope, J. *Macromolecules* **2002**, *35*, 6961–6969.
(20) McCormick, M.; Smith, R.; Graf, R.; Barrett, C.; Reven, L.; Spiess, H. *Macromolecules* **2003**, *36*, 3616–3625.
(21) Zhang, Q.; Matsukawa, S.; Watanabe, T. *Food Hydrocolloids* **2004**, *18*, 441–449.
(22) Chen, P.; Long, Z.; Ruan, R.; Labuza, T. *Lebensm-Wiss Technol.* **1997**, *30*, 178–183.
(23) Mao, R.; Tang, J.; Swanson, B. *J. Food Sci.* **2000**, *65*, 374–381.
(24) Choi, S.; Kerr, W. *Food Res. Int.* **2003**, *36*, 341–348.
(25) Lee, S.; Rho, J. *Food Sci. Biotechnol.* **2003**, *12*, 321–325.
(26) Okada, R.; Matsukawa, S.; Watanabe, T. *J. Mol. Struct.* **2002**, *602*, 473–483.
(27) Traore, A.; Foucat, L.; Renou, J. *Biopolymers* **2000**, *53*, 476–483.
(28) Vackier, M.; Hills, B.; Rutledge, D. *J. Magn. Reson.* **1999**, *138*, 36–42.
(29) Meiboom, S.; Gill, D. *Rev. Sci. Instrum.* **1958**, *29*, 688–691.
(30) Hahn, E. L. *Phys. Rev.* **1950**, *80*, 580–594.
(31) Provencher, S. W. *Comput. Phys. Commun.* **1982**, *27*, 213–217.
(32) Chen, A. W. D.; Johnson, C. s., Jr. *J. Am. Chem. Soc.* **1995**, *117*, 7965–7970.
(33) Hinton, D. P.; Johnson, C. S. *J. Phys. Chem.* **1993**, *97*, 9064–9072.
(34) Morris, K. F.; Cutak, B. J.; Dixon, A. M.; Larive, C. K. *Anal. Chem.* **1999**, *71*, 5315–5321.
(35) Morris, K. F.; Johnson, C. S.; Wong, T. C. *J. Phys. Chem.* **1994**, *98*, 603–608.
(36) ASTM (2002c). *Annual book of ASTM standards*; American Society for Testing and Materials: Philadelphia, PA, 2002; pp 1048–1053.
(37) ASTM (2002a). *Annual book of ASTM standards*; American Society for Testing and Materials: Philadelphia, PA, 2002; pp 472–477.
(38) Hills, B. P. *Mol. Phys.* **1992**, *76*, 489–508.
(39) Hills, B. P. *Mol. Phys.* **1992**, *76*, 509–523.
(40) Aliev, A. *Biopolymers* **2005**, *77*, 230–245.
(41) Kim, Y.; Cornillon, P. *Lebensm-Wiss. Technol.* **2001**, *34*, 417–423.
(42) Choi, S.; Kim, K.; Hanna, M.; Weller, C.; Kerr, W. *J. Food Sci.* **2003**, *68*, 2516–2522.
(43) Ross, Y.; Karel, M. *Biotechnol. Prog.* **1990**, *6*, 159–163.
(44) Levine, H.; Slade, L. *Carbohyd. Polym.* **1986**, *6*, 213–244.
(45) Cuq, B.; Gontard, N.; Guilbert, S. *Polymer* **1997**, *38*, 2399–2405.
(46) Arvanitoyannis, I. S. In *Protein-based films and coatings*; Gennadios, A., Ed.; CRC Press: Boca Raton, FL, 2002; pp 275–304.
(47) Tanner, S. F.; Hills, B. P.; Parker, R. *J. Chem. Soc., Faraday Trans.* **1991**, *87*, 2613–2621.
(48) Slichter, C. P. *Principles of magnetic resonance*; Springer-Verlag: Berlin, 1990.
(49) Hore, P. J. *Nuclear magnetic resonance*; Oxford University Press: New York, 1995.
(50) Ratkovic, S.; Pissis, P. *J. Mater. Sci.* **1997**, *32*, 3061–3068.
(51) Kou, Y.; Dickinson, L. C.; Chinachoti, P. *J. Agric. Food Chem.* **2000**, *48*, 5489–5495.
(52) Xin, M.; Li, M.; Yao, K. *Macromol. Symp.* **2003**, *200*, 191–197.
(53) Muramatsu, M.; Okura, M.; Kuboyama, K.; Ougizawa, T.; Yamamoto, T.; Nishihara, Y.; Saito, Y.; Ito, K.; Hirata, K.; Kobayashi, Y *Radiat. Phys. Chem.* **2003**, *68*, 561–564.
(54) Peppas, N. A.; Huang, Y.; Torres-Lugo, M.; Ward, J. H.; Zhang, J. *Annu. Rev. Biomed. Eng.* **2000**, *2*, 9–29.
(55) Hannig, M.; Dobbert, A.; Stigler, R.; Muller, U.; Prokhorova, S. A. *J. Nanosci. Nanotechnol.* **2004**, *4*, 532–538.

Received for review April 13, 2007. Revised manuscript received September 21, 2007. Accepted September 24, 2007.

JF071092F